2019 IEEE/RSJ International Conference on Intelligent Robots and Systems (IROS)
Macau, China, November 4-8, 2019

On the effect of semielliptical foot shape on the energetic efficiency of passive bipedal gait*

Aikaterini Smyrli, Mehdi Ghiassi, Andrés Kecskeméthy, and Evangelos Papadopoulos, *Fellow, IEEE*

***Abstract*— This paper studies the effects of varying rollover curvature on the passive dynamic gait of a biped walker. The dynamic model of a compliant biped robot is extended with the implementation of semielliptical feet, to mimic human rolling-radius progression during a step. The process of modeling the semielliptical foot shape and integrating its kinematics to the biped's dynamics is presented in detail. The passive dynamic behavior of the biped for elliptic feet of various dimensions is investigated through numerical simulations to provide results about gait stability, walking speed, energetic efficiency, and impact force levels. The concept of energetic efficiency in passive walking is discussed thoroughly, and an efficiency comparison methodology is proposed. Finally, it is shown that the biomimetically-inspired semielliptical foot profile can lead to higher gait efficiency. The results of this study can be used to optimize energetic efficiency in biped walking machines and/or gait assisting prosthetic equipment by means of foot shape optimization.**

I. INTRODUCTION

The study of human gait has been a common area of interest for the fields of robotics and biomechanics for a long time. From a robotics point of view, human kinesiology provides observation opportunities and inspiration for the development of walking machines. On the other end, robotics can provide a theoretical understanding of the underlying mechanisms governing human gait, as well as guidelines for mimicking the naturally occurring dynamics. Their successful pairing can give rise to comfortable gait-assisting prosthetic equipment and efficient walking robots.

A special mode of bipedal locomotion is passive bipedal walking. This walking mode, first presented in [1] has been a key point of interest, as it proves that walking is a natural mode of a biped's passive dynamics, achieved without the need for any kind of control.

The simplest passive biped model includes massless, rigid legs, carrying a mass at the hip joint [2][3][4]. This model has been extended in various studies: by the introduction of foot geometry and hip joint friction [1], leg compliance [5] and leg damping [6]. Various works have investigated the effects of design parameter selection on important gait characteristics, such as gait stability [7], walking speed [8], and energy dissipation [9].

Most of the recent work on passive walking assumes a semicircular foot shape [1][6][7][8][9]. This notion has been supported by studies on the rollover characteristics of human gait, reporting a high degree of resemblance between gaits achieved on circular foot profiles and human walking data [10][11].

However, studies on human kinesiology suggest that the rollover curvature in human walking varies during the foot-to-ground rolling progression, with a "functional" radius obtaining a maximum value when the foot is flat on the ground, but a minimum value at the heel-strike and toe-off events [12][13].

In an effort to mimic this behavior, a few studies have modelled passive gait on alternative foot shapes. In [14] a simplified flat foot geometry has been assumed: their biped rolls around its "heel pivot", effectively having a point-foot shape, until the "toe pivot" hits the ground with an impact, and the motion continues with the point contact moved to the front of the foot. In another study, the varying curvature effect is introduced by a piecewise polynomial function, leading to a leg geometry similar to the one observed in humans [15]. However, the rolling kinematics are once again solved by breaking down the foot geometry to a finite number of pivot points, introducing small impacts at each solution step. The impacts introduced by both methods in reality are not present in human walking, limiting the generalization of the studies' results.

To the best of our knowledge, no method of incorporating the exact kinematics of the foot-to-ground variable-curvature rolling contact in a passive dynamic biped walker has been published to date.

In this paper, a passive walking model incorporating elastic and damping elements along its legs as well as circular feet, firstly introduced in [7], is extended to investigate the passive mechanisms induced by semielliptical foot shapes, see Fig. 1.

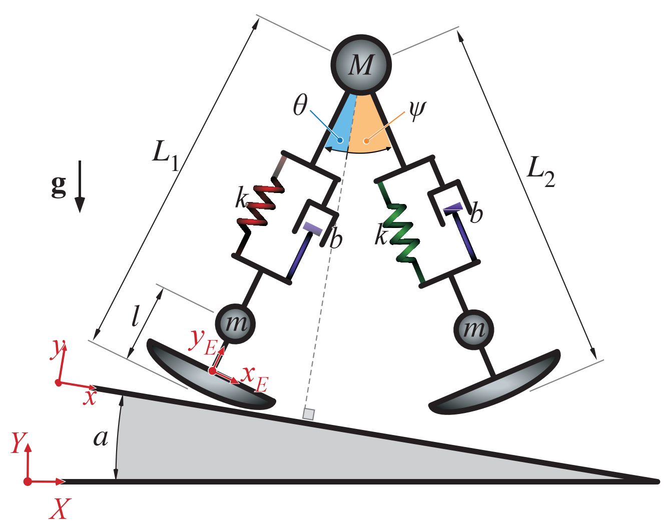

Figure 1. Passive biped model.

*Support by the German Academic Exchange Service (Deutsche Akademische Austauschdienst - DAAD) program: *Perspectives for Control of Complex Robots* DAAD HPG16 project is acknowledged.

A. Smyrli and E. Papadopoulos are with the School of Mechanical Engineering, National Technical University of Athens, (e-mail: egpapado@central.ntua.gr, tel: +30 210-772-1440). M. Ghiassi and A. Kecskeméthy are with the Faculty of Engineering, University of Duisburg-Essen.

The variable-curvature elliptic foot shape provides a certain curvature when the foot is "flat" on the ground, but a different curvature at the beginning and end of the foot-ground contact, emulating the rolling radius progression recorded in human gait. This model is studied for its passive behavior, to investigate the effects of the variable-curvature foot shapes on the energetics of walking.

The paper consists of four sections. The biped model is presented in Section II, where the focus is turned towards the analytical modeling of the semielliptical foot shape and its interface with the ground, as well as the integration of the foot's kinematics with the rest of the biped's dynamics. In Section III, the developed model is studied for its passive behavior, the notion of energetic efficiency in stable passive walking is discussed and re-defined, and useful guidelines are drawn regarding the relationship between foot shape and energetic efficiency. Finally, Section IV presents the conclusions and sets the directions for future work.

II. Passive Biped Modeling

A passive biped model, as is shown in Fig. 1, is employed. The biped performs passive walking in the *x*-direction of the *x*-*y* coordinate system (CS) of Fig. 1, which has negative slope *a*. The model consists of two elastic legs of initial length L_{nat}: the legs' elastic and damping constants are *k* and *b* respectively. The biped's body mass *M* is located at the hip joint, and the legs' inertial properties are introduced through the leg mass *m*, located at a distance *l* from the bottom of each foot. The biped is situated inside a gravity field of acceleration **g** in the -*Y* direction of the global *X*-*Y* CS. The x_E-y_E coordinate system is a local CS attached to the leg in contact with the ground.

The assumptions set to study the biped are the following: (i) the contact of the feet and ground is non-compliant, (ii) the feet perform rolling without slipping on the ground and (iii) scuffing of the swing foot during its forward advancement in the single stance phase is ignored.

A. *Generalized coordinates and system state*

The configuration of the biped is fully described by four generalized variables: the stance and swing leg angles, θ and ψ, and their corresponding leg lengths, L_1 and L_2. These compose the generalized vector **q**:

$$\mathbf{q} = \left[\theta, L_1, \psi, L_2\right]^T \qquad (1)$$

which along with its derivative, $\dot{\mathbf{q}}$, form the state vector **x** fully describing the system state:

$$\mathbf{x} = \left[\mathbf{q};\dot{\mathbf{q}}\right] = \left[\theta, L_1, \psi, L_2, \dot{\theta}, \dot{L}_1, \dot{\psi}, \dot{L}_2\right]^T \qquad (2)$$

The dynamics of the biped must be expressed with respect to the elements of the state vector: therefore, the foot kinematics must be expressed in terms of the elements of **x**.

B. *Elliptic foot geometry*

The special case of a biped model having semicircular feet has been studied in [7]. For a biped with circular feet of radius *r*, the motion of each foot rolling on the ground is described by:

$$x_r = r\theta \qquad (3)$$

where x_r is the foot center's displacement in the *x*-direction.

To mimic human anatomy and to study the effects of varying foot curvature on passive walking, in this work the biped's feet are assumed to have a *semielliptical* shape. This change in foot shape complicates the analytical description of the rolling motion of the feet on the ground.

Fig. 2 presents the elliptical foot shape on the foot-bound x_E-y_E CS, see Fig. 1. An ellipse in this plane is made up of points of the form:

$${}^E(x_i, y_i) = (r_a \cos\varphi_c, r_b \sin\varphi_c) \qquad (4)$$

where r_a and r_b are the ellipse's major and minor radii on the x_E and y_E axes respectively, and φ_c is a parameter visualized as the angle of a line whose intersections with two circles of radius r_a and r_b result in the (x_i, y_i) coordinates of each ellipse point, as is shown in Fig. 2. This point on the ellipse determines the geometric angle φ_e, for which:

$$\tan\varphi_e = \frac{y_i}{x_i} = \frac{r_b \sin\varphi_c}{r_a \cos\varphi_c} = \frac{r_b}{r_a}\tan\varphi_c \qquad (5)$$

This last equation links a geometric point (x_i, y_i) of the ellipse's perimeter to the parameter φ_c used in the definition of the ellipse, enabling the expression of contact geometry through simple algebraic equations.

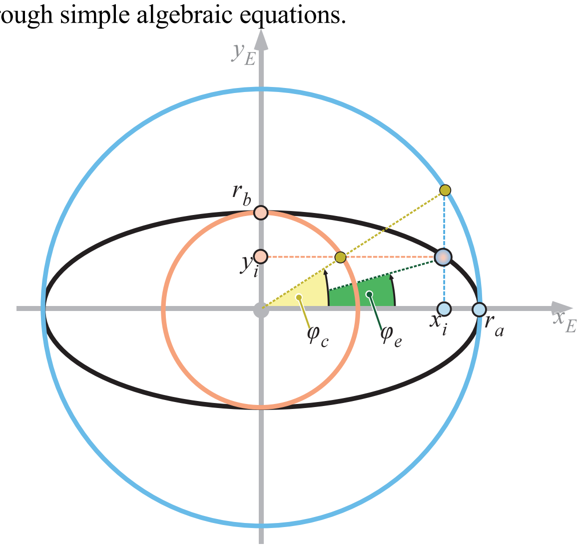

Figure 2. Elliptic foot geometry.

C. *Contact geometry in terms of state variables*

In Fig. 3, the elliptic foot is tangent to the ground at the point of contact. Therefore, for a foot rotation angle θ, see Fig. 3, the tangent to the ellipse at the contact point, measured in the x_E-y_E CS, can be calculated using the definition of the tangent line for Eq. (4):

$$\tan\theta = {}^E\left|\frac{dy_i}{dx_i}\right. = \frac{dy_i}{d\varphi_c}\frac{d\varphi_c}{dx_i} = \frac{(r_b\cos\varphi_c)}{(-r_a\sin\varphi_c)} = \frac{-r_b}{r_a\tan\varphi_c} \qquad (6)$$

providing a relationship between φ_c and θ. Therefore, at the contact point, φ_e can be linked to the leg angle θ using (5):

$$\tan\theta = \frac{-r_b^{\,2}}{r_a^{\,2}\tan\varphi_e} \qquad (7)$$

D. *The kinematics of rolling on elliptic feet*

The elliptic foot of Fig. 3 performs rolling without slipping on flat ground: by increasing the leg angle from 0 to

θ, the resulting displacement of the contact point, x_{roll} must be equal to the ellipse's arc length x_e:

$$x_{roll} \triangleq x_e = \int_{-\pi/2}^{\varphi_c} \sqrt{\left(r_a \sin\varphi\right)^2 + \left(r_b \cos\varphi\right)^2}\, d\varphi \quad (8)$$

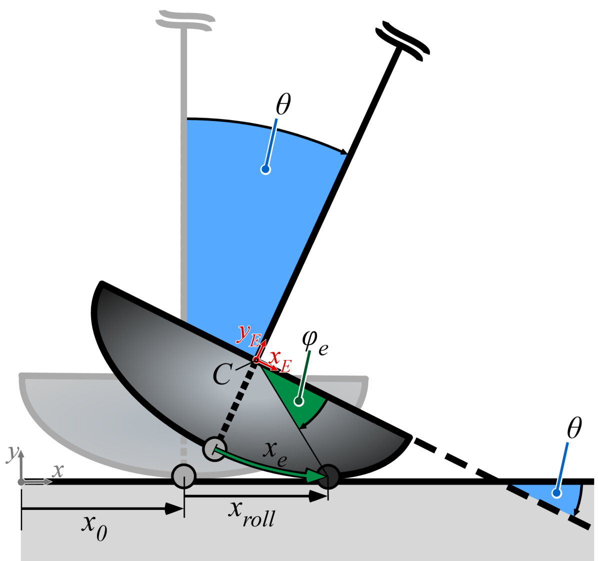

Figure 3. Rolling without slipping for the elliptic foot.

Knowing x_{roll}, it is possible to express the position of the center of the ellipse, C, in x-y coordinates:

$$x_C = x_0 + x_{roll} - \cos(\theta - \varphi_e)\sqrt{\left(r_a \cos\varphi_c\right)^2 + (r_b \sin\varphi_c)^2} \quad (9)$$

$$y_C = \sin(\theta - \varphi_e)\sqrt{\left(r_a \cos\varphi_c\right)^2 + (r_b \sin\varphi_c)^2} \quad (10)$$

In (9), x_0 is the distance of the contact point from the origin when θ=0, as is shown in Fig. 3. Note that φ_e, φ_c<0 for the bottom part of the ellipse, where contact occurs.

The spatial configuration of the rest of the biped can be expressed with respect to point C's coordinates. Note that the x-y CS is rotated by $a<0$ with respect to the global CS; therefore, both x_c and y_c are used for the estimation of the biped's potential energy due to gravity **g** in the X-Y CS. The Lagrangian will then contain the integral x_{roll}, introduced through the potential energy terms. This integral does not have an analytical solution; however, only the time and state derivatives of x_{roll} are used to produce the dynamic equations of the biped in the Lagrangian formulation. These are produced via the chain rule and can be expressed analytically:

$$\frac{dx_{roll}}{d\theta} = \frac{dx_{roll}}{d\varphi_c}\frac{d\varphi_c}{d\theta} = \frac{r_a r_b}{\sqrt{\left(r_a \sin\varphi_c\right)^2 + \left(r_b \cos\varphi_c\right)^2}} \quad (11)$$

$$\dot{x}_{roll} = \frac{dx_{roll}}{d\theta}\dot{\theta} \quad (12)$$

Therefore, the differential equations describing the state of the biped can be analytically expressed as a function of the state variables in **x**, bypassing the limitation introduced by x_{roll} in (8) not having a closed-form analytical expression.

E. *Single stance phase*

During the *single stance phase* of walking (SSP), only one of the biped's feet, called the *stance* foot, is in contact with the ground, while the *swing* foot advances forward.

The biped's motion is governed by a set of four non-linear second-order dynamic equations, which can be expressed in the form:

$$\mathbf{M(q)\ddot{q} + C(q,\dot{q})\dot{q} + K(q) + G(q) = 0} \quad (13)$$

where $\mathbf{M}_{4x4}$ is the inertia matrix of the system, $\mathbf{C}_{4x4}$ introduces centrifugal, Coriolis and damping terms, $\mathbf{K}_{4x1}$ is a vector containing the spring forces, and $\mathbf{G}_{4x1}$ is the gravity vector.

The system (13) is solved by MATLAB's moderately-stiff `ode23t` solver for its initial-condition response to the state at the beginning of the nth step, $\mathbf{x_n}$.

The SSP ends when the swing foot hits the ground, at the heel strike event (HS), with a state vector $\mathbf{x_{n,HS}}$. The HS event is triggered when three conditions are met simultaneously: these are the foot-on-ground condition (14), the swing leg advancement condition (15), and the swing leg retraction condition (16):

$$y_{C1} + (L_1 - b)\cos\theta - (L_2 - b)\cos\psi - y_{C2} = 0 \quad (14)$$

$$\psi > 0 \quad (15)$$

$$\dot{\psi} < 0 \quad (16)$$

In (14) the subscripts "1" and "2" refer to the stance and swing leg respectively. It is worth noting that x_{C2} and y_{C2} emerge from (9) and (10) by using the angle -ψ in place of θ.

The initial state $\mathbf{x_n}$ is mapped to the state at HS, $\mathbf{x_{n,HS}}$ through the dynamics in (13); this mapping can be written in the form of a discrete function f_1:

$$\mathbf{x_{n,HS}} = f_1(\mathbf{x_n}) \quad (17)$$

F. *Double stance phase*

When the swing foot hits the ground at the end of the SSP, both legs are in rolling contact with the ground, and the biped is in the *double stance phase* (DSP). This configuration constrains two of the system's degrees of freedom (DOF), by introducing two more equations that must be satisfied by the biped's state: these are the no slip condition (18) and the foot-on-ground condition (19):

$$s_1 = x_{C1} + (L_1 - b)\sin\theta + (L_2 - b)\sin\psi - x_{C2} = 0 \quad (18)$$

$$s_2 = y_{C1} + (L_1 - b)\cos\theta - (L_2 - b)\cos\psi - y_{C2} = 0 \quad (19)$$

The equations of motion governing the DSP are of the form:

$$\begin{gathered} \mathbf{M(q)\ddot{q} + C(q,\dot{q})\dot{q} + K(q) + G(q) - \Pi(q)\lambda = 0} \\ \mathbf{s} = \begin{bmatrix} s_1(\mathbf{q}) \\ s_2(\mathbf{q}) \end{bmatrix} = \mathbf{0} \end{gathered} \quad (20)$$

In (20) $\mathbf{\Pi}_{4x2}$ is the transpose of the constraint Jacobian:

$$\mathbf{\Pi(q)} = \left(\frac{\partial \mathbf{s}}{\partial \mathbf{q}}\right)^T \quad (21)$$

while $\boldsymbol{\lambda}_{2x1}$ is a vector containing the Lagrange multipliers for the satisfaction of the constraints, **s**.

The dynamical system (20) contains both differential and algebraic equations (DAE). In order to obtain a system of differential equations, the constraint equations **s=0** in (20) would have to be differentiated twice: therefore, the DAE system would be of index 2.

To solve this index 2 DAE system, the constraints $\mathbf{s}=\mathbf{0}$ are differentiated once to obtain:

$$\begin{gathered}\mathbf{M}(\mathbf{q})\ddot{\mathbf{q}}+\mathbf{C}(\mathbf{q},\dot{\mathbf{q}})\dot{\mathbf{q}}+\mathbf{K}(\mathbf{q})+\mathbf{G}(\mathbf{q})-\mathbf{\Pi}(\mathbf{q})\boldsymbol{\lambda}=\mathbf{0}\\ \dot{\mathbf{s}}=\mathbf{0}\end{gathered} \tag{22}$$

The system in (22) is now a DAE system of index 1. The new constraints translate to $\mathbf{s}=\text{const.}$, and since $\mathbf{s}=\mathbf{0}$ at HS, see (14), the constraints **s=0** are satisfied by the solution of (22). MATLAB's solver `ode15s` is used to solve the DAE system (22) for its response to the initial conditions $\mathbf{x}_{\mathbf{n,HS}}$.

The DSP terminates when the stance leg is lifted from the ground: to detect this instant, the ground forces are calculated with a Newton-Euler approach. The instance when the normal ground force on the stance leg becomes zero marks the toe-off event (TO), with a state of $\mathbf{x}_{\mathbf{n,TO}}$.

The DSP process can also be described by the discrete function f_2 in a manner similar to (17):

$$\mathbf{x}_{\mathbf{n,TO}}=f_2(\mathbf{x}_{\mathbf{n,HS}})=f_2(f_1(\mathbf{x}_{\mathbf{n}})) \tag{23}$$

G. *Transition between steps*

The state at the beginning of the (n+1)$^{\text{th}}$ step, $\mathbf{x}_{\mathbf{n+1}}$, emerges from the multiplication of $\mathbf{x}_{\mathbf{n,TO}}$ with the transformation matrix $\mathbf{T}_{\mathbf{8x8}}$:

$$\mathbf{x}_{\text{n+1}}=\mathbf{T}\mathbf{x}_{\text{n,TO}} \tag{24}$$

which flips the stance and swing leg initial conditions to prepare for the next step. The elements of **T** are all zero except for $t_{15}=t_{26}=t_{51}=t_{62}=-1$ and $t_{37}=t_{48}=t_{73}=t_{84}=1$. The negative elements of **T** are due to the convention of defining the leg angles in opposite directions, as seen in Fig. 1.

H. *Fixed points and gait stability*

The process described by (17), (23) and (24) can be summarized by (25):

$$\mathbf{x}_{\text{n+1}}=\mathbf{T}f_2(f_1(\mathbf{x}_{\text{n}}))\triangleq\mathbf{P}(\mathbf{x}_{\text{n}}) \tag{25}$$

where **P** is a discrete function describing a full step of the biped. A fixed point of **P**, $\mathbf{x}^*$, constitutes a fully repetitive gait and is defined by (26):

$$\mathbf{x}^*=\mathbf{P}(\mathbf{x}^*) \tag{26}$$

A Newton-Raphson numerical method is used to find such gaits:

$$\mathbf{x}_n^{\langle k+1\rangle}=\mathbf{x}_n^{\langle k\rangle}+v(\mathbf{I}_{8\text{x}8}-\nabla\mathbf{P}(\mathbf{x}_n^{\langle k\rangle}))^{-1}[\mathbf{P}(\mathbf{x}_n^{\langle k\rangle})-\mathbf{x}_n^{\langle k\rangle}] \tag{27}$$

In (27) v is a relaxation parameter, used to regulate the solution steps of the solver as **P** is highly nonlinear: setting v=1 as in the original method, might prohibit the convergence of the solver towards the solution, since the Jacobian $\nabla\mathbf{P}$ can obtain large values. With this in mind, (27) is repeatedly solved until numerical convergence, according to the following empirical convergence criterion:

$$\left\|\mathbf{x}_{\text{n}}^{<k+1>}-\mathbf{x}_{\text{n}}^{<k>}\right\|_\infty<10^{-6} \tag{28}$$

The stability of a fixed-point $\mathbf{x}^*$ of **P** can be estimated by linearizing **P** around $\mathbf{x}^*$:

$$\Delta\mathbf{x}^*_{\text{n+1}}=\left.\frac{\partial\mathbf{P}(\mathbf{x}^*)}{\partial\mathbf{x}}\right|_{\mathbf{x}=\mathbf{x}^*}\Delta\mathbf{x}^*_{\text{n}}\triangleq\mathbf{A}\Delta\mathbf{x}^*_{\text{n}} \tag{29}$$

where $\mathbf{\Delta x}=\mathbf{x}-\mathbf{x}^*$, a small variation of the biped state from its calculated fixed point. The eigenvalues $\mathbf{e}_{\mathbf{8x1}}$ of $\mathbf{A}_{\mathbf{8x8}}$ characterize the gait stability: the system is stable around the fixed-point $\mathbf{x}^*$ if all elements of **e** have a magnitude smaller than 1, i.e. they lie inside the unit circle in the z-domain.

III. Passive Gait on Slope

A nominal biped design with semicircular feet has been optimized for its passive gait stability in [7], by finding **e** for different biped configurations that lead to different functions **P**. The design parameters of the nominal biped are listed in Table I.

In the semicircular feet scenario, the two elliptic radii r_a and r_b are equal to each other and set to r. In this special case, the radius of curvature is constant throughout the step.

TABLE I. Nominal Biped Parameters.

Parameter	Explanation	Nominal Value
M	Biped body mass	80 [kg]
L_{nat}	Natural leg length	1 [m]
a	Floor slope	-2°
b	Damping constant	909.56 [Ns/m]
k	Elastic constant	23309 [N/m]
l	Foot mass distance	0.1485 [m]
m	Foot mass	1.296 [kg]
r_a	Elliptic radius in x_E	0.363 [m]
r_b	Elliptic radius in y_E	0.363 [m]

A. *Passive walking on semielliptical feet*

To investigate the effects of semielliptical foot shape on passive walking, fixed points were determined for bipeds of varying foot shapes by changing the values of the elliptic radii on the nominal biped of Table I. The radii r_a and r_b were gradually increased from 0 to 0.4 [m]: all possible combinations of the two were examined, to produce various foot shapes, ranging from "pointy" feet of large r_b, to "flattened" feet of large r_a, visualized schematically in Fig. 4.

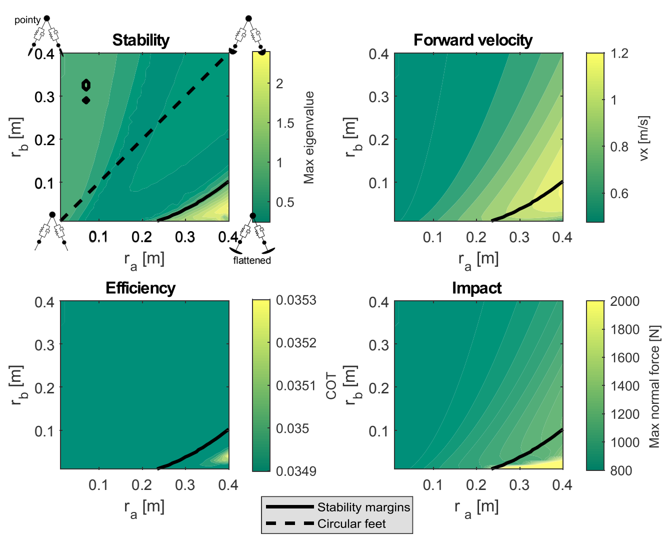

Figure 4. Energetic distribution in passive walking. Continuous black lines indicate the limits of the stable region.

The resulting bipeds' passive gaits were evaluated for their stability, forward velocity, energetic efficiency and impact force levels, and the results were plotted in Fig. 4.

In the stability chart of Fig. 4, it is shown that the passive gaits of bipeds with circular feet (where $r_a= r_b$, marked with a dashed diagonal line in the stability chart), are generally stable; the same holds for bipeds with pointy feet with $r_b> r_a$; however, bipeds with longer, flattened feet of $r_a<r_b$ perform less stable passive walks. By observing the velocity and impact force plots of Fig. 4 it can be deduced that flattened foot profiles result in faster gaits, with larger impact loads during the ground contact.

In general, changes in r_a appear to affect the gait characteristics more drastically in comparison to changes in r_b, which is apparent due to the steeper slope in the direction of r_a in most of the plots of Fig. 4. The pointy foot shapes in feet of larger r_b behave in the same manner as the actual point-foot case, obtained when $r_a=r_b=0$. However, the semielliptical feet tend to become longer and flatter when r_a increases, making it difficult for the passive biped to lift its feet above the ground before HS.

However, the energetic efficiency remains the same for all stable walks, regardless of the foot shape. This observation is intuitive for repetitive gaits but must be further investigated before reaching any conclusions on the relationship between foot shape and energetic efficiency.

B. *Energy considerations in passive walking*

The stable passive descendance of a biped walking on a negative slope is only possible due to energy conservation. The energetic losses of the biped due to its intrinsic damping elements as well as due to the impacts with the ground are compensated by the potential energy obtained by its descent through the gravity field.

Fig. 5 presents the energy distribution for a biped walking on a negative slope. It can be seen that the kinetic as well as the elastic energy of the biped at each instant are oscillating around a fixed average value during the passive walk, indicating the repetitiveness of the gait.

The gravitational potential energy presents a decreasing trend as the biped descends towards the negative *Y*-direction of Fig. 1, while the total energy lost through damping presents an increasing trend as the dissipation power due to the dampers and ground impacts is accumulated. The sum of the above energetic components, plotted in the last plot of Fig. 5, is shown to be constant during each step as a direct consequence of energy conservation. The sum only decreases with a discontinuity at each HS instance: this is a consequence of the conservation of angular momentum of the system before and after the HS event. The discontinuity step of the plot is then equal to the amount of energy lost due to the impact of the foot with the ground at HS.

The Cost of Transport (COT) of any walking machine is defined as the ratio of the energy loss during a walk over the product of the machine's weight with the distance it travelled:

$$\mathrm{COT} = \frac{E_{out}}{Mg\Delta x} \tag{30}$$

where E_{out} is the energy loss due to damping and ground impacts, and Δx is a distance traveled in the *x*-direction of Fig. 1.

However, for the gait to be repetitive, the total energy must be conserved, and therefore the energy output must equal the energy input, E_{in}.

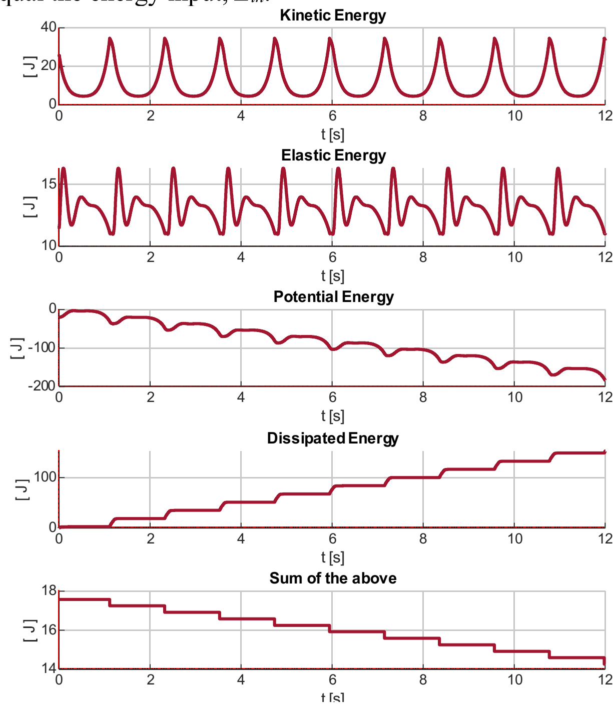

Figure 5. Energetic distribution in passive walking.

In passive walking, E_{in} originates from the energetic gain due to the descent $\Delta Y = \Delta x \sin a$, therefore:

$$\mathrm{COT} = \frac{E_{in}}{Mg\Delta x} = \frac{|Mg\Delta x \sin a|}{Mg\Delta x} = |\sin a| \tag{31}$$

The convergence of the COT as defined in (30) towards the theoretical value of (31) for a passive biped commencing its gait near a stable fixed point is shown in Fig. 6. It can be observed that as the gait progresses, the COT converges to $|\sin a| = 0.39$ (for $a = -2^\circ$), as a direct consequence of the energetic equilibrium in the stable system.

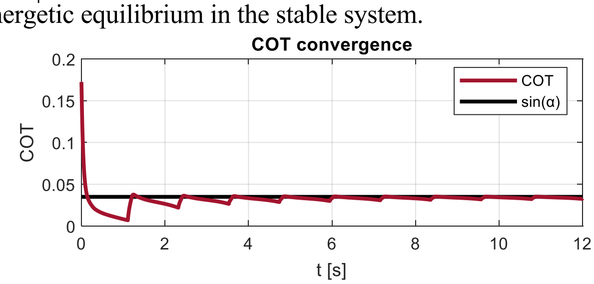

Figure 6. COT convergence to sin(a) in passive walking.

Therefore, during the use of passive walking simulations with the aim to investigate questions related to energetic consumption, it should be considered that the ground slope α directly determines the energy loss rate of the gait by means of introducing a pre-determined COT. This exact gait can then be reproduced on level ground with suitable actuation schemes [7], effectively eliminating the slope a, and the COT of the active gait will theoretically be that of (31).

To restate, the angle a of the slope should only be treated as a direct measure of COT, and target-oriented comparisons should be used for energetic efficiency considerations in passive walking through elimination of a. Here we select to investigate the effect of foot shape on energy efficiency with respect to a targeted forward gait velocity.

C. *Foot shape and gait efficiency*

According to the above observations, we select a target forward velocity of v_x =0.6 [m/s]. The question of energetic efficiency can then be posed as follows: Is it possible to design a foot shape that will decrease the amount of energy needed to perform a walk for the target v_x?

To answer this last question, the slope angle of the passive walker is decreased to smaller values, therefore decreasing the COT of all stable passive gaits achieved on the new slopes. Then the foot-shape investigation process presented in Fig. 4 is repeated for the biped on the smaller slopes. The contour levels of gaits with the target forward velocity v_x =0.6 [m/s] are extracted from the corresponding velocity contour plots and re-plotted in Fig. 7, where a is eliminated and the COT acts as a plotting parameter.

The lower-COT dashed curves in Fig. 7 are on the right of the higher-COT curves, corresponding to larger elliptic radii r_a. It is then clear that for a targeted forward gait velocity, less pointy foot shapes, associated with larger r_a for a certain r_b, allow for lower COT, and therefore for larger energy efficiency during the gait.

This observation has potential extensions to the biomechanics of gait, implying that the human foot configuration, where the foot is flat on the ground for a large portion of each step, might have evolved towards optimizing the energetic efficiency of the most common mode of human locomotion, which is bipedal walking.

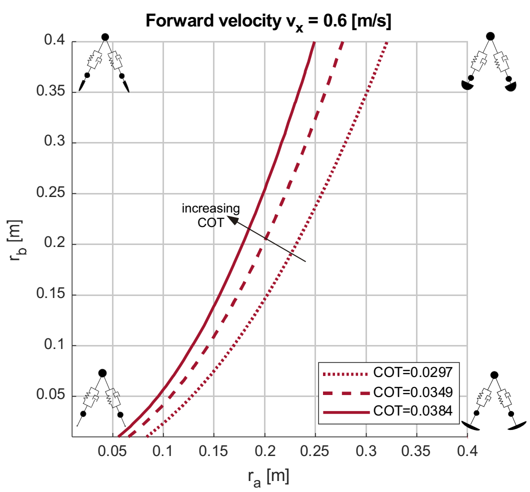

Figure 7. Constant forward gait velocity contours for different foot shapes.

IV. Conclusion

A passive biped model was extended with the addition of semielliptical feet, to mimic human rolling curvature progression. The methods followed to produce the kinetics of the semielliptical foot shape, the analytic expression of its rolling contact with the ground, and the integration of the above to the full biped's dynamics were thoroughly presented. The passive gait of the biped on semielliptical feet was studied for its stability, velocity, energetic efficiency and heel-strike impact force levels. The energy distribution of the biped throughout its passive gait was studied and the energetic efficiency of all stable passive bipeds walking on a given slope was proven to only be dependent on that slope.

Following the above, a first step was made towards reconfiguring the criteria and methods used for energetic comparisons between passive walking models. Finally, it was shown that flattened foot shapes can lead to gaits of better energy efficiency for a targeted walking speed. This translates to lower metabolic effort when walking on natural or prosthetic feet of variable foot curvature, as well as lower actuation power for walking robots having this foot design.

A future extension of this study is to develop a general methodology for the simulation of various foot shapes, defined either by a specific function or even a random series of points. This will allow the comparison of several foot shapes, unconstrained by the elliptic profile assumed here.

References

[1] McGeer, T., "Passive Dynamic Walking", *The International Journal of Robotics Research*, 1990. 9(2): pp. 62-82.

[2] Garcia, M., et al., "The Simplest Walking Model: Stability, Complexity, and Scaling," *Journal of Biomechanical Engineering*, 1998, 120(2): pp. 281-288.

[3] Kuo, A. D., "Energetics of actively powered locomotion using the simplest walking model", *Journal of Biomechanical Engineering*, 2002, 124(1): pp. 113-120.

[4] Gregg, R. D., et al., "On the mechanics of functional asymmetry in bipedal walking," *IEEE Transactions on Biomedical Engineering*, 2012, 59(5): pp.1310-1318.

[5] Alexander, R., "A model of bipedal locomotion on compliant legs", *Philosophical Transactions of the Royal Society of London, Series B: Biological Sciences*, 1992, 338(1284): pp. 189-198.

[6] Linde, R.Q.V.D., "Active leg compliance for passive walking," *IEEE International Conference on Robotics and Automation (ICRA '98),* Leuven, Belgium, 1998, pp. 2339-2344.

[7] Smyrli, A., Bertos, G. and Papadopoulos, E., "Efficient stabilization of zero-slope walking for bipedal robots following their passive fixed-point trajectories.", *IEEE International Conference on Robotics and Automation (ICRA)*, Brisbane, Australia, 2018, pp. 5733-5738.

[8] Asano, F. and Luo, Z.W., "On Energy-Efficient and High-Speed Dynamic Biped Locomotion with Semicircular Feet", *IEEE/RSJ Int. Conf. on Intelligent Robots & Systems (IROS '98),* Beijing, China, 2006, pp. 5901-5906.

[9] Asano, F. and Luo, Z.W. "The effect of semicircular feet on energy dissipation by heel-strike in dynamic biped locomotion," *IEEE International Conference on Robotics and Automation (ICRA '07),* Rome, Italy, 2007, pp. 3976-3981.

[10] Gard, S.A. and Childress, D.S., "What Determines the Vertical Displacement of the Body During Normal Walking?", *Journal of Prosthetics and Orthotics*, 2001, 13(3): pp. 64-67.

[11] Adamczyk, P.G., and Kuo, A.D., "Mechanical and energetic consequences of rolling foot shape in human walking", *Journal of Experimental Biology*, 2013, 216(14): pp. 2722-2731.

[12] Caspers, L., Lugrís, U. and Kecskeméthy, A., "Foot-ground sagittal rolling behaviour during heel contact and its approximation by an exponential-curvature disk", *4th Joint International Conference on Multibody System Dynamics*, Montreal, Canada, 2016.

[13] Caspers, L., Siebler, M., Hefter, H., Lugrís, U., & Kecskeméthy, A., "Using Kinematic Rolling Surfaces for Fast Foot-Ground Modeling in the Forward Dynamics of Human Gait—A Sagittal Plane Analysis", *ECCOMAS Thematic Conference on Multibody Dynamics*, Prague, Czech Republic, 2017.

[14] Kwan, M., and Hubbard, M., "Optimal foot shape for a passive dynamic biped", *Journal of Theoretical Biology*, 2007, 248(2): pp. 331-339.

[15] Mahmoodi, P., Ransing, R.S., and Friswell, M.I., "Modelling the effect of 'heel to toe'roll-over contact on the walking dynamics of passive biped robots", *Applied Mathematical Modelling*, 2013, 37(12-13): pp. 7352-7373.